ICEF2003-729

A MODELLING APPROACH TO THE DESIGN OPTIMIZATION OF CATALYTIC CONVERTERS OF I. C. ENGINES

Ming Chen, Karen Schirmer
DCL International Inc.
P.O. Box 90, Concord, Ontario, Canada, L4K 1B2

ABSTRACT

In this paper, a modelling approach to the design optimization of catalytic converters is presented. The first step of the optimization is the model-assisted sizing of catalysts. For a given inlet exhaust condition, a semi-empirical, experimentally calibrated, 0-D steady state catalyst model is employed to sort through a data base of catalysts under given restraints, yielding few successful candidates. Following this screening process, a 1-D transient plug-flow catalyst model is used to analyze the species concentrations and the temperature variation across the catalyst.

The second step deals with the flow optimization of the catalyst converter under the given geometric restraints. A commercially available CFD package is employed to simulate isothermal flow and to evaluate flow uniformity characteristics in the catalytic converter. The substrate is modelled as porous media, where viscous and initial resistances are specified via empirical formula. With the help of the CFD tool, the flow in the converter can be optimized using appropriate boundary layer control methods. In a specific example, the effects of perforated plate on the flow separation in a wide-angle diffuser are demonstrated. This paper also addresses the issue of flow resistance of perforated plates.

INTRODUCTION

The design of oxidation catalytic converters, 3-way catalytic converters and/or SCR systems involves the determination of the loading of precious metals, and washcoat formulations. Material choice, and geometric configuration of the components of exhaust systems, (including manifolds, diffusers, setting chambers, converter housings, substrates, and contractions), and the positioning of the converter in the exhaust lines are other important design aspects. Since the 1970s significant knowledge regarding the manufacturing and utilization of catalytic converters for internal combustion engines has been acquired. However, the design of catalytic converters is still more of an empirical practice than a science. The balance of the situation may need to be shifted toward the latter as the emission standards become more stringent.

Recent publications indicate that the complexity of the exhaust gas lines is increased as a result of the use of closed coupled oxidation catalysts, storage catalysts and/or particulate filters [1], and the merging of the exhaust aftertreatment with powertrain management leads to the integrated emission reduction approaches [2]. The greater complexity associated with the advanced emission control strategies leads to a desire to incorporate modelling approaches in the design process to improve the performance of products, shorten prototype development periods and reduce overall costs. A concept of catalytic converter design and thereby the role of modelling approaches is illustrated in Fig. 1.

1-D steady state plug-flow catalyst models have been widely used to predict the performance of catalytic converters [3][4]. At DCL International Inc., a 0-D and a 1-D catalyst model are employed for the catalyst sizing and performance prediction. Although these models are robust and reliable for some ranges of applications, they are not capable of dealing with complex geometries and the associated processes, i.e. multi-dimensional flow and heat transfer.

Flow maldistribution not only lowers the local Damköhler number in the higher velocity zones, but also produces larger aging effects [5] in these zones, which subsequently result in reduced overall conversion efficiency of the species. Hence, the catalyst model analysis needs to be supplemented by CFD

assisted flow optimization under the given geometric restraints. Thereby, special attention is being paid to the configurations of the diffuser, the setting chamber, the contraction section, and the layout of catalyst blocks. These components are arranged to delivery to the catalyst substrate, a flow whose velocity is as uniform as possible, besides, minimum pressure losses are produced.
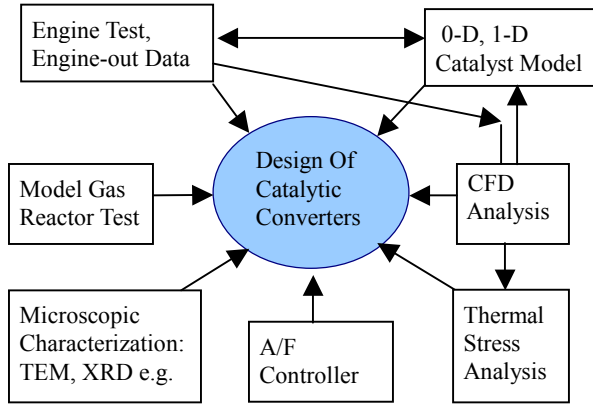

Fig.1. The role of the modeling approach for the improvement of catalytic converters and its relations with the experimental approaches.

In the following the mathematical models used in the catalyst sizing and analysis are introduced. Furthermore, some practical issues of multi-dimensional CFD modelling of catalytic converters are addressed. The effects of perforated plate on the flow separation in a wide-angle diffuser are investigated. A specific simulation example is provided to illustrate the applicability of the approach.

NOMENCLATURE

$C_{g,i}$ Gas concentration (mole fraction) of component [-]

C_{pg} Specific heat at constant pressure of gas [J/(kg K)]

C_{ps} Specific heat of solid [J/(kg K)]

C_{Pt} Specific PM loading of catalysts [g/l]

C Inertial resistance coefficient [m^{-1}]

D Viscous resistance coefficient [m^{-2}]

Da Damköhler number [-]

Ga Geometric surface area per unit substrate volume [m^2/m^3]

d Diameter of the orifices of perforated plates [m]

d_h Hydraulic diameter of the substrate [m]

h Heat transfer coefficient [J/(m^2 s K)]

ΔH Heat of reaction [mol/J]

l Thickness of the perforated [m]

L Length of catalyst [m]

k Overall reaction rate constant [1/s]

k_{ci} Intrinsic mass transfer coefficient [-]

k_{ri} Intrinsic kinetic rate coefficient [-]

K Pressure drop coefficient of screen [m/s]

$\dot{m}_g$ Exhaust mass flow [kg/s]

M_g Molecular weight of exhaust [kg/kmol]

$N_{species}$ Number of species [-]

p Pressure [Pa]

Δp Pressure drop [Pa]

R Radius of catalyst substrate [m]

S_{BET} Effective BET surface area [m^2/g]

S_i Cross-section area of i th channel of substrate [m]

v Superficial velocity [m/s]

t Time [s]

T_g Gas temperature [K]

T_s Solid temperature [K]

Y Resistance coefficient of the substrate [-]

z Axial distance [m]

Greek symbols

α Constant [-]

ε Void volume fraction [-]

γ Flow uniformity index [-]

ρ_g Gas density [kg/m^3]

ρ_s Solid density [kg/m^3]

ρ_{wc} Washcoat density [kg/m^3]

λ_s Thermal conductivity of solid [W/(m K)]

λ_g Thermal conductivity of gas [W/(m K)]

η Conversion efficiency; internal effectiveness factor [-]

μ Dynamic viscosity [kg/(m s)]

Superscript

γ Specific PM exponent; uniformity index [-]

Subscript

ave   Average

g   Gas

i   Species index; index of the channels of substrate

s   Solid

MODEL-ASSISTED SIZING OF CATALYSTS

0-D Catalyst Model

Under the assumption of a zero-dimensional, steady, isothermal reactor and first order reaction rates, an expression of the conversion efficiency of the species is given by [6]:

$$\eta = 1 - e^{-\frac{kL}{v}} \qquad (1)$$

The Damköhler number, Da, is defined as the ratio of the characteristic flow time and the characteristic reaction time. Here the former is the flow residence time and the latter is the inverse of the overall reaction rate constant. Thus the Damköhler number is expressed as:

$$Da = \frac{kL}{v} \qquad (2)$$

Then Eq. (1) is rewritten as

$$\eta = 1 - e^{-Da} \qquad (3)$$

Eq. (3) indicates that the Damköhler number is a governing parameter of the solution. A large Damköhler number corresponds to a higher conversion efficiency of the reactant.

The overall reaction rate constant is expressed as [7]:

$$\frac{1}{k} = \frac{1}{\eta\, C_{Pt}^{\gamma}\ k_{ri}\,\rho_{wc}\, S_{BET}\ c_1} + \frac{1}{Ga\ k_{ci}}. \qquad (4)$$

The first and second terms on the r.h.s. of the above equation is the inverse of the kinetic rate coefficient, and the inverse of the mass transfer coefficient, respectively. The intrinsic kinetic rate coefficient k_{ri} is calculated by an Arrhenius's expression. c_1 equals the mole fraction of the oxygen for the oxidation reactions, and equals 1 for non-oxidation reactions. The intrinsic mass transfer coefficient k_{ci} is calculated from the correlation between Sherwood number and Reynolds number. A data base of the rate constants for different species is established for a range of catalyst types, mainly through in-house catalyst tests on an engine dynamometer test bench.

For a given inlet exhaust condition, a 0-D catalyst model is employed to sort through a data base of catalyst candidates (with different material, geometrical dimensions, cell density and catalyst types) under given restraints (e.g. the maximum backpressure, the range of space velocity, and the required conversion efficiency), yielding few successful candidates.

1-D Transient Catalyst Model

Following the above screening process, a 1-D plug flow catalyst model is used to predict the concentrations of the species, and the temperature variations of the solid phase and the gas phase along the axial location of the converters. The governing equations read:

$$\varepsilon \cdot \frac{\partial C_{g,i}}{\partial t} = -v \cdot \frac{\partial C_{g,i}}{\partial z} - k \cdot Ga \cdot C_{g,i}\,, \qquad i = 1, 2, ..., N_{species} \qquad (5)$$

$$\varepsilon \cdot \rho_g \cdot C_{pg} \frac{\partial T_g}{\partial t} = -v \cdot \rho_g \cdot C_{pg} \cdot \frac{\partial T_g}{\partial z} + h \cdot Ga \cdot (T_s - T_g) \qquad (6)$$

$$(1-\varepsilon) \cdot \rho_s \cdot C_{ps} \cdot \frac{\partial T_s}{\partial t} = \lambda_s \cdot (1-\varepsilon) \cdot \frac{\partial^2 T_s}{\partial z^2} + h \cdot Ga \cdot (T_g - T_s)$$
$$+ \sum_{i=1}^{N_{species}} (-\Delta H)_i \cdot \frac{\dot{m}_g}{\pi \cdot R^2 \cdot M_g} \frac{\partial C_{g,i}}{\partial z} \qquad (7)$$

The 1-D model is useful to analyze the catalyst performance in the cases where significant transient effects and/or variations in concentrations and temperature along the axial direction exist. Typical examples are cold start or thermal runway in case of rich excursion.

FLOW ANALYSIS AND OPTIMIZATION

Theoretical Analysis of a 0-D case

A catalytic converter may be assumed as a network of parallel zero-dimensional, steady, isothermal reactors. To consider the effects of the flow distribution on the conversion efficiency of the species, we apply Eq. (3) locally for each channel of the substrate. This leads to the overall conversion efficiency:

$$\eta = 1 - \frac{\sum_i v_i \cdot S_i \cdot \exp(-Da_i)}{\sum_i v_i \cdot S_i} \qquad (8)$$

Here v_i and Da_i are the local superficial velocity and the local Damköhler number in the i th channel of the monolithic substrate, respectively. Following Eq. (2) Da_i is calculated using the local superficial velocity, with k and L unchanged.

To illustrate the influence of the flow velocity on the conversion efficiency of the species, we take an idealized example of a cylindrical catalyst substrate with a radius of one unit. We assume a velocity profile of $v_i(r) = 5 - 4r$, which corresponds to $\gamma = 0.82$, γ is the flow uniformity index, and

its definition is found in [5]. The local Damköhler number is calculated as $Da_i(r) = Da \cdot v_{ave}/(5 - 4r)$, where Da is the Damköhler number for the uniform flow case with the flow velocity equaling the average velocity v_{ave} of the non-uniform flow case. A comparison of the results between the uniform velocity case and the non-uniform velocity case is shown in Fig.2.
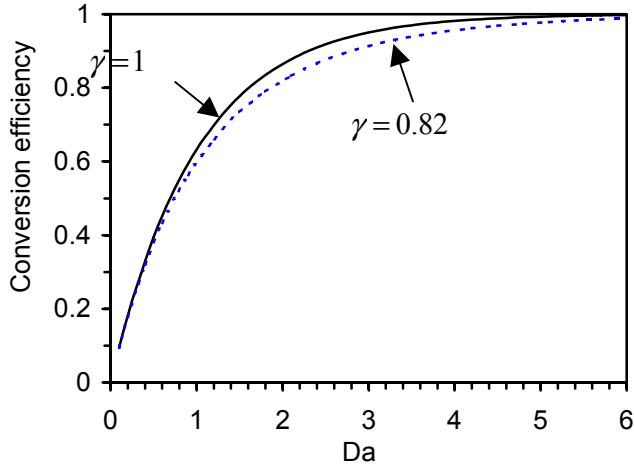

Fig.2. Conversion efficiency of the species as a function of the Damköhler number at different flow uniformity indexes.

Multi-Dimensional CFD Simulations

Flow resistance of the substrate

The actual substrate is regarded as porous media and is treated as a fictitious continuum, such enabling the use of the partial differential equations. The porous media resistance coefficients are anisotropic and are practically deduced from experiments. They are specified along three directions based on the substrate type, the cell density, the hydraulic diameter and the resistance of the substrate.

The equation for calculating local pressure drop reads:

$$\Delta P = \alpha \ \mu(T_g) \ \frac{L}{d_h^2} \ v + \frac{1}{2} \ Y \ \rho_g(T_g) \ v^2 \qquad (9)$$

The first term on the r. h. s. of the above equation is a viscous loss term. The second term, which is an inertial term, accounts for the deviation from Darcy's law. The resistance of the substrate, Y, is a function of cell density, substrate material and coating thickness. In the employed CFD software package, FLUENT, porous media are modeled by the addition of a sources term to the momentum equations of flow. The source term for the i th momentum equation reads:

$$S_i = \frac{\partial p}{\partial x_i} = -\sum_{j=1}^{3} D_{ij} \mu \, v_j - \frac{1}{2} \sum_{j=1}^{3} C_{ij} \rho \mid v_j \mid v_j \qquad (10)$$

When the direction of the i th coordinate coincides with the longitudinal direction of substrate channels, one obtains the following:

$$D_{ii} = \alpha/d_h^2 \qquad (11)$$

$$D_{jj} = D_{kk} =_{+\infty} \qquad (12)$$

$$C_{ii} = Y/L \qquad (13)$$

$$C_{jj} = C_{kk} =^{+}\infty \qquad (14)$$

The non-diagonal components of the matrices C and D are zero. Here the subscripts j and k denotes the other two coordinate directions of a Cartesian coordinate system.

The screen

Due to space and cost restraints, wide-angle diffusers are used in catalytic converters, which may cause serous flow separation. The latter can adversely influence the performance of the converters.

Gauze screens have been used in wide-angle diffusers of low speed wind tunnels to suppress flow separation and produce uniform exit flows [8]. A review on the topic of flow through screens was given by Laws and Levesey [9]. Screens facilitate a uniform velocity profile by introducing a pressure drop proportional to the square of the velocity. For the catalytic converters, a pressure drop across the screen may be acceptable when the benefits of a uniform velocity profile outweigh the disadvantage of the energy loss.

The central issue of selecting screens is the determination of the pressure drop coefficient, which is defined by:

$$K = \frac{\Delta p}{\frac{1}{2}\rho_g v^2}. \qquad (15)$$

where Δp is the pressure drop through the screen. K is dependent on the open area ratio of the screen, the geometry configuration and Reynolds number. Significant deviations of K are found between wired screens [8] [9] and sharp edged perforated plates [10][11][12]. Experimental data of K for perforated thick plates (l/d > 0.015) at high Reynolds number is found in [12]. Here l denotes the thickness of the plate, d the diameter of the orifices.

For catalytic converters, the computational effort for resolving a large number of small orifices geometrically is prohibitive. In order to predict the screen's effects on the flow distribution in the catalytic converter, a porous jump boundary condition has to be applied to represent the pressure drop through the screen. This treatment implies the assumption that the screen has no influence on the turbulence. The issue of the suppression and generation of the turbulence by the screens will not be addressed in this paper.

To study the adequacy of the simplification and to investigate the influence of the Reynolds number on K, a simulation of the steady flow through a screen with the real geometric features is performed. 9 orifices with the diameter of 4.763 mm, and a pitch of 5.935 mm are placed in line on a solid plate with a dimension of 17.8 mm × 17.8 mm × 1.65mm, resulting in an open area ratio of 51%. The inlet and outlet faces are placed upstream and downstream of the plate with a distance of 22.9 × d. The symmetry boundaries are imposed on the four sides of the domain. 786,079 non-uniform hexahedral cells are used. Turbulence is modeled by a standard k-ϵ turbulence model.

The static pressure and velocity magnitude along the center line of the orifice are shown in Fig.3. The pressure drop is established within a non-dimensional axial distance of x/d = 3.6, which correspond to 2.89% of the length of the diffuser, and is only 1.43% of the width of the screen for a large catalytic converter described in the next section. It may be concluded that it is appropriate to assume the screen as a surface of pressure discontinuity. As shown in Fig. 4, the calculated pressure drop coefficient K agrees well with that from Idel'chik at high Reynolds number [12]. K increases as Reynolds number decreases.
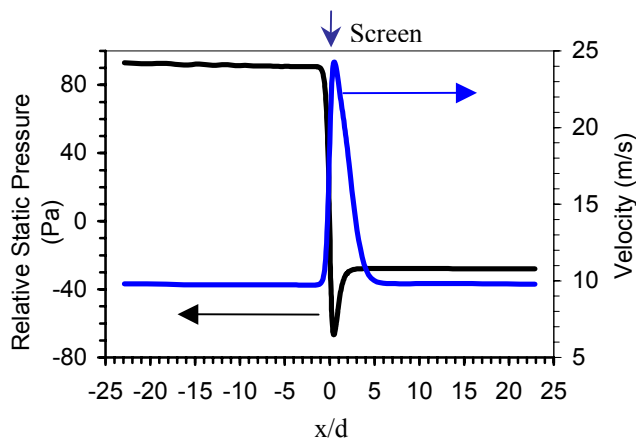

Fig. 3. The static pressure and the velocity magnitude along the centerline of the orifice.
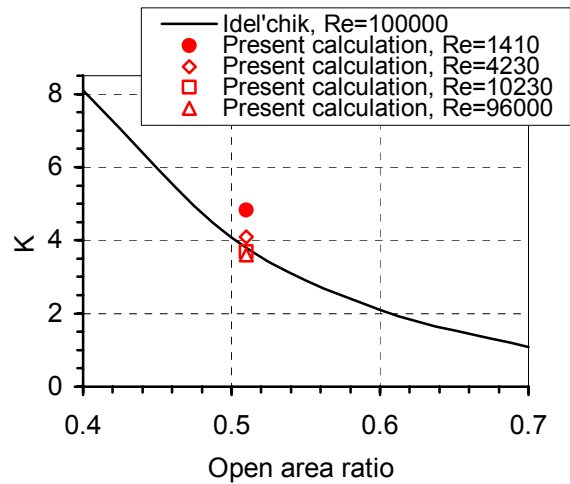

Fig. 4. The pressure drop coefficient as a function of the open area ratio (σ) and the Reynolds number $(Re= \dfrac{v \cdot d \cdot \rho}{\mu \cdot \sigma})$.

CFD Simulation of a large catalytic converter

An oxidation catalyst converter for large stationary diesel engines is chosen as a simulation example. The exhaust has a mass flow rate of 8.4 kg/s, and the gas temperature is 420 °C. The turbulent intensity and the hydraulic diameter at the inlet are 5 %, and 0.82 m respectively. There are two layers of oxidation catalysts placed in a brick shaped chamber, which is connected to cylindrical pipes through a 40° angle diffuser and a contraction section with rectangular cross sections. In the diffuser of the converter, a perforated plate is placed at an axial location of 38% of the diffuser length. For structural reasons, the perforated plate is welded on a peripheric frame. For comparison purpose, three cases as listed in Table 1, are included in the CFD analysis. The outline of the geometry and computational domain is shown in Fig.5. For case A and case B, there are 197,900 non-uniform cells, which contain hexahedral (six sided) and tetrahedral cells. For case C, more cells are used in order to resolve the added geometric feature.

Table 1. Calculation cases.

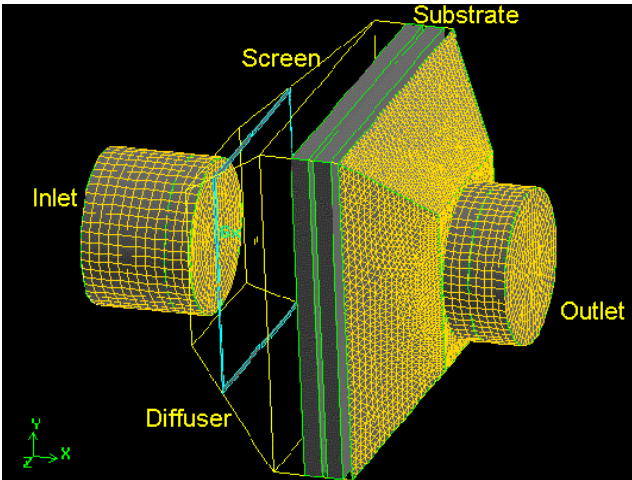| case A	without screen
case B	with one screen, 51% open area ratio, K=3.91
case C	with one screen welded on a 25.4 mm peripheric frame, 51% open area ratio, K=3.91

Fig. 5. The geometric configuration and part of the mesh.

For case A and case C, the contours of the velocity in the x direction at a symmetric cross section parallel to the direction of the inlet flow are shown in Fig. 6, and Fig. 7, respectively. For case A, the separation occurs at the wall of the diffuser, and a large recirculation zone is formed. This zone extends from the diffuser to the setting chamber. The setting chamber is located between the catalyst and the diffuser. For case C, only a small separation zone is found between the beginning of the diffuser and the location of the screen, which is visualized by velocity vectors on a close-up view near the screen in Fig. 8. Downstream of the screen, the main stream of the flow attaches to the wall.
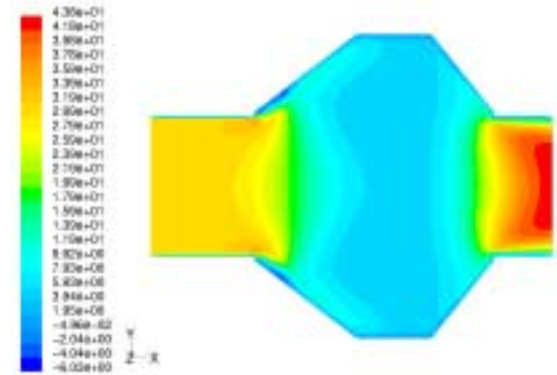

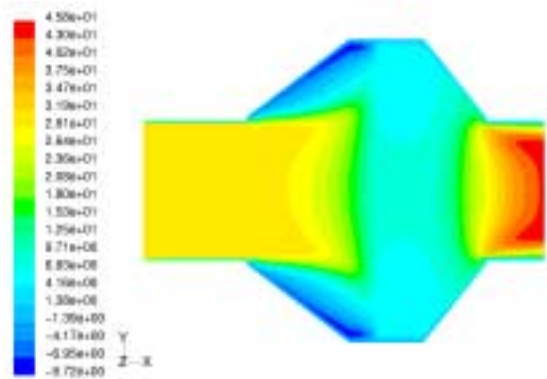Fig.6. Contours of the velocity component in x direction at the symmetric cross section in y-x plane, case A.

Fig. 7. Contours of the velocity component in the x direction at the symmetric cross section in y-x plane, case C.
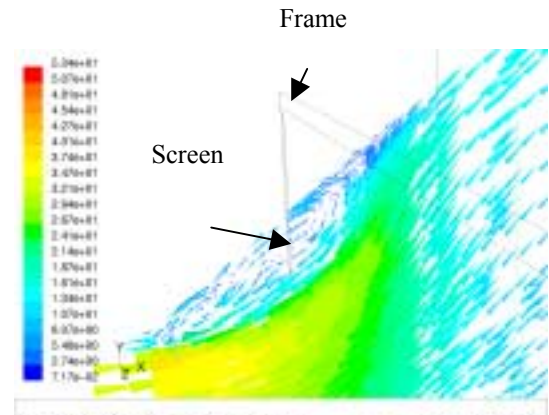

Fig. 8. Velocity vectors in the symmetric cross section in y-x plane, case C.

Table 2. The uniformity index.

Location of the cross sections	case A	case B	case C
End of the diffuser	0.670	0.908	0.887
Catalyst front face	0.856	0.976	0.966

Table 3. Area-weighted average total pressure (pa).

Location of the cross sections	case A	case B	case C
Inlet	1298	1458	1435
Catalyst front face	1157	1089	1092
Endof the diffuser	1096	1093	1100
Outlet	325	312	312

The simulations indicate that the screen is effective in removing velocity nonuniformities. Table 2 summarizes the flow uniformity index, γ, at two cross sections, one is at the end of the diffuser, and the other is at the front face of the catalyst. For the case C, γ is 0.966, which corresponds to an increase of 12.9%, compared with that of the case A.

The averaged total pressures at the cross sections of interest are given in Table 3. For the case C, in terms of the increase of the pressure drop, the penalty of using the screen is 150 Pa or 0.6 inch w.c.

CONCLUSION

The robust 0-D and 1-D catalyst sizing and analysis model needs to be supplemented by CFD analysis so that the performance of the catalytic converters can be better evaluated.

With the CFD software package, the flow uniformity index and the averaged total pressure at the interested cross section of the catalytic converters are calculated by the state of the art modeling techniques for flow resistance of the substrate and the pressure jump through the perforated plates. It has been numerically analyzed that it is reasonable to assume the perforated plate as a surface of pressure discontinuity. Through a specific simulation, it has been demonstrated that the perforated plate with an appropriate open area ratio is effective in removing velocity nonuniformities with a small penalty of pressure losses.

ACKNOWLEDGMENTS

REFERENCES

[1] Wanker, R., Granter H., Bachler, G.: New physical and chemical model for the CFD simulation of exhaust gas lines: A generic approach. SAE 2002-01-0066.

[2] Herrmann, H.O., Lang, O., Mikulic, I, Scholz, V.: Particulate filter systems for diesel passanger cars, MTZ 9/2001.

[3] Koltsakis, G. C., Konstantinidis, P. A., Stamatelos, A.M., Development and application of mathematical models for 3-way catalytic converters, Applied Catalysis B: Environment, Vol 12, p. 161-191, 1997.

[4] Laing, P. M., Shane, M. D., Son, S., Adamczyk, A. A, Li, P., A simplified approach to modelling exhaust system emissions: SIMTWC, SAE paper 1999-01-3476.

[5] Martin, A. P., Will, N. S., etc., Effect of flow distribution on emissions performance of catalytic converter, SAE paper 980936.

[6] Heck, R. M., Farrauto, R. J., Catalytic pollution control, John Wiley & Sons, Inc., 2002.

[7] Leprince, T., L., Aleixo, J., Chowdhury, K., Naseri, M., Williams, S., Development of pre-turbo catalyst for natural gas engines, Proceeding of 2003 Spring Technical Conference of the ASME Internal Combustion Engine Division Salzburg, Austria, May 11-14, 2003.

[8] Mehta, R. D. and Bradshaw, P., Design rules for small low speed wind tunnels, Aeronautical Journal of the Royal Aeronautical Society, November 1979.

[9] Laws, E.M., Livesey, J. L., Flow through screens, Ann. Rev. Fluid Mech. 1979, 10:247-66.

[10] Pinker, R. A., Herbert, M. V., Pressure losses associated with compressible flow through square-mesh wire gauzes, J. Mech. Eng. Sci. 11:290-94.

[11] Blevins, R. D., Applied fluid dynamics handbook, Van Nostrand Rhinhold Company, Inc., 1984.

[12] Idel'chik, I.E., Handbook of hydraulic resistance, 3rd ed., CRC Press, Inc., 1994.